Computers and Electrical Engineering 100 (2022) 107907

Contents lists available at ScienceDirect

Computers and Electrical Engineering

journal homepage: www.elsevier.com/locate/compeleceng

Performance analysis of cognitive hybrid radio frequency and free space optical cooperative networks☆

Dong Qin

School of Information Engineering, Nanchang University, Nanchang 330031, China

ARTICLE INFO

Keywords:
Free space optical
Higher order statistics
Ergodic capacity
Bit error probability

ABSTRACT

This paper studies the exact performance of hybrid radio frequency and free space optical cooperative amplify and forward communication networks in a cognitive radio environment, where secondary users cannot transmit signals at any power level since the existence of the primary users restrict the behavior of the secondary users within an acceptable and reasonable range. In particular, a secondary relay station connects a destination through a free space optical link, whose random characteristics follows a widely used gamma–gamma fading distribution with non zero pointing error to characterize the assignable effects of atmospheric turbulence. Different from the traditional analysis methods in probability theory based on cumulative distribution function or outage probability, the complicated integral domain division is avoided by virtue of the moment generating function of reciprocal signal to noise ratio. Under the maximum interference level constraint of the primary user, exact closed form expressions of moments of signal to noise ratio, ergodic capacity, higher order statistics of the capacity, and average bit error probability are derived naturally. Finally, simulation results are provided to flawlessly demonstrate the theoretical analysis.

1. Introduction

Recently, wireless products cannot connect to WiFi or wireless access points at will since limited spectrum resources have greatly restricted their access and application to prevent mutual interference. Therefore, the current 5G technology is moving towards higher frequencies and developing spectrum resources that have not yet been fully utilized. But higher frequency means greater attenuation, and shorter distances under the same power distribution conditions. This shortcoming is obviously not conducive to long distance transmission and communication. Thus 5G communications in higher frequency bands need to deploy more micro base stations to achieve long distance transmission. This is the duality of a coin. In this context, traditional cognitive radio technology is still one of the effective ways to relieve the tension of the spectrum. On the other hand, high rate transmission of optical communication networks just make up for the lack of spectrum bandwidth. And optical communication technology has been used to construct back haul links and front haul links for core network and macro cells. Another characteristic application is deploying optical communication for last mile access network or disaster recovery link. But a major challenge comes from the requirement of line of sight transmission in optical communications, which is difficult to always be guaranteed in existing mobile cellular systems. Therefore, combining the advantages of both free space optical (FSO) communication and radio frequency (RF) communication can provide users with better service experience and network performance. For instance, the intermittent connectivity of underwater optical wireless sensor networks was investigated in [1], where the hostile channel damage and misalignment has severely affected the propagation range of the underwater optical links. A FSO configuration was introduced into a multihop network in [2] for decode

☆ This paper is for regular issues of CAEE. Reviews processed and recommended for publication to the Editor-in-Chief by Guest Editor Dr. Robert Bstak.

E-mail address: qindong@ncu.edu.cn.

https://doi.org/10.1016/j.compeleceng.2022.107907
Received 4 July 2021; Received in revised form 6 March 2022; Accepted 10 March 2022
Available online 1 April 2022

and forward protocol with hard switching configuration under weak and strong turbulence. A physical layer security problem was studied in [3] for simultaneous wireless information and power transfer wireless optical networks, where a potential eavesdropper receive information from the source node through RF links. The ergodic capacity of multihop FSO system with RF backup was exploited in [4], where the optical link and the radio frequency link constitute a selective combination scheme. The cloud radio access network architecture was considered in [5] for FSO system, where the RF link underwent $\kappa - \mu$ shadowed fading and FSO link was modeled as the exponential Weibull distribution. The hybrid RF and FSO spectrum sharing relaying networks with energy harvesting technique was studied in [6], where the secondary user was equipped limited battery. A nonzero boresight pointing error was introduced in [7], where the FSO link is modeled as a complex double generalized gamma turbulence channel. And a partial relay selection strategy was employed in this spectrum sharing environment. The imperfect channel state information caused by channel estimation errors is analyzed in [8], where power control and symbol detection process were considered in decode and forward hybrid multiple input multiple output RF/FSO relaying system. The diversity multiplexing trade off was implemented in [9] for combined power constraint was imposed at the secondary user. The orthogonal space time block code and transmit antenna selection were studied in [10], where the characteristics of primary user node mobility was introduced in the spectrum sharing network. A varying channel condition was considered in [11], where an adaptive joint resource scheduling was optimized to guarantee better data connectivity in mixed FSO and RF network. A link budget was designed in [12] for reliable link quality for optical communication network due bad weather challenge.

Form the above literature, there are still several deficiencies. Firstly, the optical communication channel model in some documents omitted the influence of pointing errors for simplicity [11–13]. Although this simplified the channel modeling process, it cannot be applied to more complex environments. Obviously, the fewer factors to be considered, the simpler calculation process and complexity. But it is impossible to be zero pointing error in optical communication transmission under the influence of atmospheric turbulence. Secondly, while a good understanding of spectrum sharing strategies in cognitive radio technology has been fully provided in the previous works about hybrid RF and FSO systems, integer parameters m are still habitually assumed as a common choice in Nakagami-m environment for RF links [3,6]. Recent studies have shown that the integer parameter is chosen only for the convenience of calculation without considering the actual situation, because it can be expanded into a summation form with finite terms without affecting the precision of the theoretical values. This operation is equivalent to replacing a complex function with several simple functions. But this may not be true in a complex and changeable wireless environment. From a practical point of view, the choice of integer parameter m cannot characterize versatile fading scenarios. Finally, in the derivation of closed form solutions, the previous works often listed integral formulas and then looked up the corresponding integral table [4,5]. However, this method is not suitable for the cognitive cooperative system, because the closed-form solution cannot be found in complex optical communication channels by this method.

Inspired by the above observations, a detailed and comprehensive performance analysis is discussed about the impact of spectrum sharing technology on hybrid RF and FSO amplify and forward (AF) relaying systems. The contribution of this paper lies in the following aspects. (1) The precise performance analysis of hybrid RF and FSO communication systems based on spectrum sharing is achieved by assuming Nakagami-m fading with arbitrary parameter m for RF link and gamma–gamma channel model with atmosphere turbulence for FSO link. (2) Discarding the common series expansion method due to calculation of complicated definite integral in finite domain, the moment generating function of the reciprocal signal to noise ratio (SNR) is used to obtain the closed expression of important performance metrics such as the moment of the SNR, ergodic capacity, higher order statistics of the capacity and average bit error probability (BEP). (3) Moreover, the secondary relay station is assumed to suffer from the interference of the cochannel signals, which is often overlooked in the spectrum sharing environment. Importantly, such newly obtained formulas are suitable for arbitrary fading parameter m, the strength of the atmospheric turbulence and the number of interference signals.

The remainder of this paper is organized as follows. System model is given in Section 2. Performance analysis is presented in Section 3. Simulation results are showed in Section 4. Finally, conclusion is drawn in Section 5.

2. System model

Consider a spectrum sharing environment where a primary network opens a section of spectrum to the secondary network in the surrounding neighborhood, as show in Fig. 1. A primary transmitter PS and a primary receiver PD constitute the primary network architecture. While the secondary network is a typical cooperative network, consisting of a secondary source SS, a secondary relay station SR and a secondary destination SD. Denote h_{sr} as the channel coefficient of $SS \to SR$. Let h_{sp} be the interference channel coefficient of $SS \to PD$ since the secondary user has to open its own transmitter to send signals. Due to the broadcasting characteristics of RF transmission, secondary users can easily access the authorized spectrum without being physically close to the primary user. But this does not mean that the behavior of secondary users is not restricted and constrained. The secondary is allowed to access the spectrum only if the quality of service of the primary network is guaranteed. Therefore, the power of the secondary user SS has to be adjusted to $p_s = QN_0/\left|h_{sp}\right|^2$, where Q is the tolerable threshold the primary user can endure and N_0 is the noise variance. Different from the integer fading parameter assumption of previous work, here all RF links h_{sr} and h_{sp} are supposed to undergo Nakagami-m fading with arbitrary parameter including integers and non integers. For ease of reference, a list of abbreviations is listed in Table 1.

Furthermore, assume that the relay station suffers from the interference of I cochannel signals, $h_{I,1}, h_{I,2}, \ldots, h_{I,I}$. According to the criterion of the AF protocol, the equivalent SNR at the relay station SR is given by

$$\gamma_1 = \frac{p_s \left|h_{sr}\right|^2}{\sum_{i=0}^{I} \left|h_{I,i}\right|^2} = \frac{Q \left|h_{sr}\right|^2 N_0}{\left|h_{sp}\right|^2 \left(\sum_{i=0}^{I} \left|h_{I,i}\right|^2\right)} \tag{1}$$

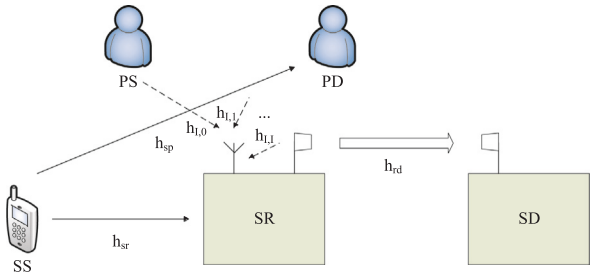

Fig. 1. System model.

Table 1
List of abbreviations.

Acronyms	Descriptions
AF	Amplify and forward
BEP	Bit error probability
DD	Direct detection
FSO	Free space optical
IM	Intensity modulation
PD	Primary destination receiver
PS	Primary source transmitter
RF	Radio frequency
SD	Secondary destination
SNR	Signal to noise ratio
SR	Secondary relay station
SS	Secondary source

where $h_{I,0}$ represents the interference from the primary user PS. In order to simplify the analysis, it is assumed that all cochannel interference signals obey independent and identical Nakagami distribution. Note that if a nonidentical distribution is assumed, the sum of all interfering signals can still be approximated to a Nakagami distribution [14].

On the other hand, the FSO link between the relay station SR and the destination node SD depends on atmospheric turbulence and pointing error, whose probability distribution function is given by [15]

$$f_{\gamma_2}(z) = \frac{\xi^2}{r\Gamma(a)\Gamma(b)z} G_{1,3}^{3,0}\left[hab\left(\frac{z}{\mu_r}\right)^{\frac{1}{r}} \middle| \begin{matrix} \xi^2+1 \\ \xi^2, a, b \end{matrix}\right] \tag{2}$$

where ξ is the ratio between the equivalent beam radius of the wave and the standard deviation of the pointing error displacement at the receiver, $h = \xi^2/\left(\xi^2+1\right)$. The quality r specifies the detection type being used, i.e., $r = 1$ denotes heterodyne detection and $r = 2$ shows intensity modulation/direct detection (IM/DD). a and b are scintillation and fading parameters related to the atmospheric turbulence conditions. The quality γ_2 is the equivalent electrical SNR at SD. $G(\cdot)$ is the Meijer's G function [16, eq.(9.301)]. The parameter μ_r is the average SNR of the FSO link defined as [1]

$$\mu_r = \begin{cases} E\left(\gamma_2\right) & r = 1 \\ \frac{E(\gamma_2)ab\xi^2\left(\xi^2+2\right)}{(a+1)(b+1)\left(\xi^2+1\right)^2} & r = 2 \end{cases} \tag{3}$$

where $E(\cdot)$ is expectation operation.

3. Performance analysis

In terms of the AF protocol process, the overall SNR is given by

$$\gamma = \frac{\gamma_1\gamma_2}{\gamma_1+\gamma_2} \tag{4}$$

Before analyzing the overall SNR γ, the statistical behavior of the variable γ_1 has to be calculated first. According to the law of the probability of random variable, the cumulative distribution function of γ_1 is given by

$$\begin{aligned} F_{\gamma_1}(u) &= \int_0^{+\infty}\int_0^{+\infty}\int_0^{uyz} f_{Q|h_s|^2}(x) f_{|h_p|^2}(y) f_{\sum_{i=0}^{I}|h_{I,i}|^2}(z)\, dx dy dz \\ &= 1 - \frac{1}{\Gamma\left(m_{s,1}\right)\Gamma\left(m_{s,2}\right)\Gamma\left(m_{s,3}\right)} H_{3,2}^{2,2}\left[\frac{\beta_{s,1}z}{\beta_{s,2}\beta_{s,3}} \middle| \begin{matrix} \left(1-m_{s,2},1\right),\left(1-m_{s,3},1\right),(1,1) \\ (0,1),\left(m_{s,1},1\right) \end{matrix}\right] \end{aligned} \tag{5}$$

where $f_x(\cdot)$ represents the probability distribution function of variable x, $m_{s,1}$, $m_{s,2}$ and $m_{s,3}$ are the respective fading severity parameters of $SS \to SR$ link, $SS \to PD$ link and interfering signal links, $\beta_{s,1}$, $\beta_{s,2}$ and $\beta_{s,3}$ are the corresponding scale parameters. $\Gamma(\cdot)$ and $H(\cdot)$ denote the gamma function [16, eq.(8.310)] and Fox's H function [17, eq.(1.1.1)], respectively. Because all RF links obey the Nakagami-m distribution, the channel gains follow the gamma distribution, whose probability distribution function can be found in many literature, such as [18]. Differentiating the cumulative distribution function yields the probability distribution function of γ_1 given by

$$f_{\gamma_1}(u) = \frac{dF_{\gamma_1}(u)}{du} = \frac{H_{2,1}^{1,2}\left[\frac{\beta_{s,1}u}{\beta_{s,2}\beta_{s,3}}\middle| \begin{matrix}(1-m_{s,2},1),(1-m_{s,3},1)\\ (m_{s,1},1)\end{matrix}\right]}{u\Gamma(m_{s,1})\Gamma(m_{s,2})\Gamma(m_{s,3})} \tag{6}$$

3.1. Moment generating function

If the statistical behavior of the SNR γ is extrapolated directly from the perspective of probability theory, serial expansion has to be resorted to in terms of the characteristics of the gamma function. When the fading severity parameter is an integer, the series expansion of the finite term can be obtained fortunately. But when the severity parameter is not an integer, an infinite series will appear. In order to avoid the uncertainty and instability of the infinite series, the moment generating function of the reciprocal SNR is adopted. Using the identity [17, eq.(2.8.4)], the moment generating function of the reciprocal SNR γ_1 is given by

$$\begin{aligned} M_{\frac{1}{\gamma_1}}(s) &= E\left(e^{-\frac{s}{x}}\right) = \int_0^{+\infty} e^{-\frac{s}{x}} f_{\gamma_1}(x)\,dx \\ &= \int_0^{+\infty} \frac{e^{-\frac{s}{x}}}{x\Gamma(m_{s,1})\Gamma(m_{s,2})\Gamma(m_{s,3})} H_{2,1}^{1,2}\left[\frac{\beta_{s,1}x}{\beta_{s,2}\beta_{s,3}}\middle| \begin{matrix}(1-m_{s,2},1),(1-m_{s,3},1)\\ (m_{s,1},1)\end{matrix}\right] dx \\ &= \frac{H_{2,2}^{2,2}\left[\frac{\beta_{s,1}s}{\beta_{s,2}\beta_{s,3}}\middle| \begin{matrix}(1-m_{s,2},1),(1-m_{s,3},1)\\ (m_{s,1},1),(0,1)\end{matrix}\right]}{\Gamma(m_{s,1})\Gamma(m_{s,2})\Gamma(m_{s,3})} \end{aligned} \tag{7}$$

where the exponential function is expressed in terms of Fox's H function given by [17, eq.(2.9.4)]

$$\frac{e^{-\frac{s}{x}}}{x} = \frac{H_{0,1}^{1,0}\left[\frac{s}{x}\middle| \begin{matrix}-\\ (0,1)\end{matrix}\right]}{x} = \frac{H_{1,0}^{0,1}\left[\frac{x}{s}\middle| \begin{matrix}(0,1)\\ -\end{matrix}\right]}{s} \tag{8}$$

Similarly, the moment generating function of the reciprocal SNR γ_2 is given by

$$\begin{aligned} M_{\frac{1}{\gamma_2}}(s) &= E\left(e^{-\frac{s}{x}}\right) = \int_0^{+\infty} e^{-\frac{s}{x}} f_{\gamma_2}(x)\,dx \\ &= \int_0^{+\infty} \frac{e^{-\frac{s}{x}}\xi^2}{r\Gamma(a)\Gamma(b)x} G_{1,3}^{3,0}\left[hab\left(\frac{x}{\mu_r}\right)^{\frac{1}{r}}\middle| \begin{matrix}\xi^2+1\\ \xi^2,a,b\end{matrix}\right] dx \\ &= \frac{\xi^2 H_{1,4}^{4,0}\left[\frac{(hab)^r s}{\mu_r}\middle| \begin{matrix}(\xi^2+1,r)\\ (\xi^2,r),(a,r),(b,r),(0,1)\end{matrix}\right]}{\Gamma(a)\Gamma(b)} \end{aligned} \tag{9}$$

According to the property of the moment generating function, the moment generating function of the sum of two random variables is equal to the product of their respective moment generating functions. Hence, the moment generating function of $1/\gamma$ is given by

$$\begin{aligned} M_{\frac{1}{\gamma}}(s) &= M_{\frac{1}{\gamma_1}}(s) M_{\frac{1}{\gamma_2}}(s) \\ &= \frac{\xi^2 H_{2,2}^{2,2}\left[\frac{\beta_{s,1}s}{\beta_{s,2}\beta_{s,3}}\middle| \begin{matrix}(1-m_{s,2},1),(1-m_{s,3},1)\\ (m_{s,1},1),(0,1)\end{matrix}\right]}{\Gamma(m_{s,1})\Gamma(m_{s,2})\Gamma(m_{s,3})\Gamma(a)\Gamma(b)} H_{1,4}^{4,0}\left[\frac{(hab)^r s}{\mu_r}\middle| \begin{matrix}(\xi^2+1,r)\\ (\xi^2,r),(a,r),(b,r),(0,1)\end{matrix}\right] \end{aligned} \tag{10}$$

The moment generating function of the reciprocal SNR is a powerful tool with which many important performance metrics can be related. For example, the moment generation function relationship between a random variable and its reciprocal is discovered in [19], which is a integral formula related to Bessel function given by

$$\begin{aligned} M_\gamma(s) &= 1 - 2\sqrt{s}\int_0^{\infty} J_1\left(2\sqrt{s}x\right) M_{\frac{1}{\gamma}}\left(x^2\right) dx \\ &= 1 - \frac{\xi^2}{\Gamma(m_{s,1})\Gamma(m_{s,2})\Gamma(m_{s,3})\Gamma(a)\Gamma(b)} \\ &\quad \times H_{2,(2:1),0,(2:4)}^{1,2,0,2,4}\left[\begin{matrix}\frac{\beta_{s,1}}{\beta_{s,2}\beta_{s,3}s}\\ \frac{(hab)^r}{\mu_r s}\end{matrix}\middle| \begin{matrix}(1,1),(0,1)\\ (1-m_{s,2},1),(1-m_{s,3},1);(\xi^2+1,r)\\ -\\ (m_{s,1},1),(0,1);(\xi^2,r),(a,r),(b,r),(0,1)\end{matrix}\right] \end{aligned} \tag{11}$$

where J_1 is the Bessel function of the first kind [16, eq.(8.41)] and $H(x, y)$ is the bivariable Fox's H function [20, eq.(2.2.1)].

3.2. Moments of signal to noise ratio

The moments of SNR can be used to measure the strength of the received SNR at the destination. Sometimes, moments of SNR can also be used to compute the approximate ergodic capacity according to Jensen's inequality [21]. Using [13, Eq. (37)], the nth moment is given by

$$\begin{aligned} E(\gamma^n) &= \frac{1}{(n-1)!}\int_0^\infty s^{n-1} M_{\frac{1}{\gamma}}(s)\, ds \\ &= \frac{\mu_r^n \xi^2}{(n-1)!\,(hab)^{nr}\,\Gamma\left(m_{s,1}\right)\Gamma\left(m_{s,2}\right)\Gamma\left(m_{s,3}\right)\Gamma(a)\Gamma(b)} \\ &\quad \times H_{6,3}^{2,6}\left[\frac{\beta_{s,1}\mu_r}{\beta_{s,2}\beta_{s,3}(hab)^r}\middle| \begin{matrix}\left(1-m_{s,2},1\right),\left(1-m_{s,3},1\right),\left(1-\xi^2-nr,r\right),(1-a-nr,r),(1-b-nr,r),(1-n,1)\\ \left(m_{s,1},1\right),(0,1),\left(-\xi^2-nr,r\right)\end{matrix}\right] \end{aligned} \tag{12}$$

3.3. Ergodic capacity

One of the advantages of the optical communication system is high rate and its ergodic capacity is written by

$$\begin{aligned} E\left[\frac{1}{2}\log_2(1+c\gamma)\right] &= \frac{1}{2\ln 2}\int_0^\infty \frac{1-e^{-s}}{s} M_{\frac{1}{\gamma}}\left(\frac{s}{c}\right) ds = \frac{1}{2\ln 2}\int_0^\infty H_{1,2}^{1,1}\left[s\middle|\begin{matrix}(0,1)\\(0,1),(-1,1)\end{matrix}\right] M_{\frac{1}{\gamma}}\left(\frac{s}{c}\right) ds \\ &= \frac{\xi^2\mu_r c}{2\ln 2\,(hab)^r\,\Gamma\left(m_{s,1}\right)\Gamma\left(m_{s,2}\right)\Gamma\left(m_{s,3}\right)\Gamma(a)\Gamma(b)} \\ &\quad \times H_{4,(2:1),1,(2:2)}^{4,2,1,2,1}\left[\begin{matrix}\frac{\beta_{s,1}\mu_r}{\beta_{s,2}\beta_{s,3}(hab)^r}\\ \frac{\mu_r c}{(hab)^r}\end{matrix}\middle|\begin{matrix}\left(\xi^2+r,r\right),(a+r,r),(b+r,r),(1,1)\\ \left(1-m_{s,2},1\right),\left(1-m_{s,3},1\right);(0,1)\\ \left(\xi^2+1+r,r\right)\\ \left(m_{s,1},1\right),(0,1);(0,1),(-1,1)\end{matrix}\right] \end{aligned} \tag{13}$$

where $c = 1$ for heterodyne detection and $c = e/(2\pi)$ for IM/DD.

The concept of high-order statistics of capacity was first proposed in [22] and spread quickly. According to the definition, the nth order statistics of capacity is approximately given by

$$\begin{aligned} E(S^n) = E\left[\frac{1}{2^n}\log_2^n(1+c\gamma)\right] &\approx \sum_{k=0}^{n}\frac{(-1)^k C_n^k}{2\,(2\ln 2\Delta)^n} \\ &\int_0^{+\infty}\left[{}_1F_1(1+k\Delta;1;-s)+(-1)^n\,{}_1F_1(1-k\Delta;1;-s)\right] \\ &\times\left[M_{\frac{1}{\gamma}}\left(\frac{s}{c}\right)-\frac{\partial M_{\frac{1}{\gamma}}\left(\frac{s}{c}\right)}{\partial s}\right] ds \end{aligned} \tag{14}$$

where ${}_1F_1(\cdot)$ is called confluent hypergeometric function [16, eq.(9.210.1)] and Δ is a small number. Using [17, eq.(2.2.1)], the partial derivative of the moment generating function is given by

$$\begin{aligned} M_{\frac{1}{\gamma}}\left(\frac{s}{c}\right)-\frac{\partial M_{\frac{1}{\gamma}}\left(\frac{s}{c}\right)}{\partial s} &= \frac{\xi^2 H_{2,2}^{2,2}\left[\frac{\beta_{s,1}s}{\beta_{s,2}\beta_{s,3}c}\middle|\begin{matrix}\left(1-m_{s,2},1\right),\left(1-m_{s,3},1\right)\\ \left(m_{s,1},1\right),(0,1)\end{matrix}\right] H_{1,4}^{4,0}\left[\frac{(hab)^r s}{\mu_r c}\middle|\begin{matrix}\left(\xi^2+1,r\right)\\ \left(\xi^2,r\right),(a,r),(b,r),(0,1)\end{matrix}\right]}{\Gamma\left(m_{s,1}\right)\Gamma\left(m_{s,2}\right)\Gamma\left(m_{s,3}\right)\Gamma(a)\Gamma(b)} \\ &+\frac{\xi^2 H_{2,2}^{2,2}\left[\frac{\beta_{s,1}s}{\beta_{s,2}\beta_{s,3}c}\middle|\begin{matrix}\left(1-m_{s,2},1\right),\left(1-m_{s,3},1\right)\\ (1,1),\left(m_{s,1},1\right)\end{matrix}\right] H_{1,4}^{4,0}\left[\frac{(hab)^r s}{\mu_r c}\middle|\begin{matrix}\left(\xi^2+1,r\right)\\ \left(\xi^2,r\right),(a,r),(b,r),(0,1)\end{matrix}\right]}{\Gamma\left(m_{s,1}\right)\Gamma\left(m_{s,2}\right)\Gamma\left(m_{s,3}\right)\Gamma(a)\Gamma(b)\,s} \\ &+\frac{\xi^2 H_{2,2}^{2,2}\left[\frac{\beta_{s,1}s}{\beta_{s,2}\beta_{s,3}c}\middle|\begin{matrix}\left(1-m_{s,2},1\right),\left(1-m_{s,3},1\right)\\ \left(m_{s,1},1\right),(0,1)\end{matrix}\right] H_{1,4}^{4,0}\left[\frac{(hab)^r s}{\mu_r c}\middle|\begin{matrix}\left(\xi^2+1,r\right)\\ (1,1),\left(\xi^2,r\right),(a,r),(b,r)\end{matrix}\right]}{\Gamma\left(m_{s,1}\right)\Gamma\left(m_{s,2}\right)\Gamma\left(m_{s,3}\right)\Gamma(a)\Gamma(b)\,s} \end{aligned} \tag{15}$$

Then using [20, eq.(2.5.1)], the nth order statistics of capacity is approximately given by

$$E(S^n) \approx \sum_{k=0}^{n}\frac{(-1)^k C_n^k}{2\,(2\ln 2\Delta)^n}\int_0^{+\infty}\left[\frac{H_{1,2}^{1,1}\left[s\middle|\begin{matrix}(-k\Delta,1)\\(0,1),(0,1)\end{matrix}\right]}{\Gamma(1+k\Delta)}+(-1)^n\right.$$

$$\times\frac{H_{1,2}^{1,1}\left[s\middle|\begin{matrix}(k\Delta,1)\\(0,1),(0,1)\end{matrix}\right]}{\Gamma(1-k\Delta)}\Bigg]\Bigg[M_{\frac{1}{\gamma}}\left(\frac{s}{c}\right)-\frac{\partial M_{\frac{1}{\gamma}}\left(\frac{s}{c}\right)}{\partial s}\Bigg]ds$$

$$=\sum_{k=0}^{n}\frac{(-1)^k C_n^k \xi^2}{2(2\ln 2\Delta)^n\Gamma\left(m_{s,1}\right)\Gamma\left(m_{s,2}\right)\Gamma\left(m_{s,3}\right)\Gamma(a)\Gamma(b)}$$

$$\times\Bigg\{\frac{\mu_r c}{\Gamma(1+k\Delta)(hab)^r}\Bigg[H_{4,(1:2),1,(2:2)}^{4,1,2,1,2}\left[\begin{matrix}\frac{\mu_r c}{(hab)^r}\\\frac{\beta_{s,1}\mu_r}{\beta_{s,2}\beta_{s,3}(hab)^r}\end{matrix}\middle|\begin{matrix}\left(\xi^2+r,r\right),(a+r,r),(b+r,r),(1,1)\\(-k\Delta,1);\left(1-m_{s,2},1\right),\left(1-m_{s,3},1\right)\\\left(\xi^2+1+r,r\right)\\(0,1),(0,1);\left(m_{s,1},1\right),(0,1)\end{matrix}\right]$$

$$+H_{4,(1:2),1,(2:2)}^{4,1,2,1,2}\left[\begin{matrix}\frac{\mu_r c}{(hab)^r}\\\frac{\beta_{s,1}\mu_r}{\beta_{s,2}\beta_{s,3}(hab)^r}\end{matrix}\middle|\begin{matrix}\left(\xi^2+r,r\right),(a+r,r),(b+r,r),(1,1)\\(-k\Delta-1,1);\left(1-m_{s,2},1\right),\left(1-m_{s,3},1\right)\\\left(\xi^2+r+1,r\right)\\(-1,1),(-1,1);\left(m_{s,1},1\right),(1,1)\end{matrix}\right]$$

$$+H_{4,(1:2),1,(2:2)}^{4,1,2,1,2}\left[\begin{matrix}\frac{\mu_r c}{(hab)^r}\\\frac{\beta_{s,1}\mu_r}{\beta_{s,2}\beta_{s,3}(hab)^r}\end{matrix}\middle|\begin{matrix}\left(\xi^2+r,r\right),(a+r,r),(b+r,r),(2,1)\\(-k\Delta-1,1);\left(1-m_{s,2},1\right),\left(1-m_{s,3},1\right)\\\left(\xi^2+1+r,r\right)\\(-1,1),(-1,1);\left(m_{s,1},1\right),(0,1)\end{matrix}\right]\Bigg]$$

$$+\frac{(-1)^n\mu_r c}{\Gamma(1-k\Delta)(hab)^r}\Bigg[H_{4,(1:2),1,(2:2)}^{4,1,2,1,2}\left[\begin{matrix}\frac{\mu_r c}{(hab)^r}\\\frac{\beta_{s,1}\mu_r}{\beta_{s,2}\beta_{s,3}(hab)^r}\end{matrix}\middle|\begin{matrix}\left(\xi^2+r,r\right),(a+r,r),(b+r,r),(1,1)\\(k\Delta,1);\left(1-m_{s,2},1\right),\left(1-m_{s,3},1\right)\\\left(\xi^2+1+r,r\right)\\(0,1),(0,1);\left(m_{s,1},1\right),(0,1)\end{matrix}\right]$$

$$+H_{4,(1:2),1,(2:2)}^{4,1,2,1,2}\left[\begin{matrix}\frac{\mu_r c}{(hab)^r}\\\frac{\beta_{s,1}\mu_r}{\beta_{s,2}\beta_{s,3}(hab)^r}\end{matrix}\middle|\begin{matrix}\left(\xi^2+r,r\right),(a+r,r),(b+r,r),(1,1)\\(k\Delta-1,1);\left(1-m_{s,2},1\right),\left(1-m_{s,3},1\right)\\\left(\xi^2+r+1,r\right)\\(-1,1),(-1,1);\left(m_{s,1},1\right),(1,1)\end{matrix}\right]$$

$$+H_{4,(1:2),1,(2:2)}^{4,1,2,1,2}\left[\begin{matrix}\frac{\mu_r c}{(hab)^r}\\\frac{\beta_{s,1}\mu_r}{\beta_{s,2}\beta_{s,3}(hab)^r}\end{matrix}\middle|\begin{matrix}\left(\xi^2+r,r\right),(a+r,r),(b+r,r),(2,1)\\(k\Delta-1,1);\left(1-m_{s,2},1\right),\left(1-m_{s,3},1\right)\\\left(\xi^2+r+1,r\right)\\(-1,1),(-1,1);\left(m_{s,1},1\right),(0,1)\end{matrix}\right]\Bigg]\Bigg\} \tag{16}$$

3.4. Average bit error probability

The average BEP is one of the important indicators for judging the quality of a wireless communication system. Whether the destination receiver can decode correctly with a greater probability is the guarantee for the successful data transmission. When binary modulation scheme is used, the average BEP of the optical communication system is given by [13, Eq. (38)]

$$P_e=E\left[\frac{\Gamma(p,q\gamma)}{2\Gamma(p)}\right]=-\frac{1}{2\Gamma(p)}\int_0^\infty G_{1,3}^{2,0}\left[qs\middle|\begin{matrix}1\\p,0,0\end{matrix}\right]\frac{\partial M_{\frac{1}{\gamma}}(s)}{\partial s}ds$$

$$=\frac{1}{2}-\frac{1}{2\Gamma(p)}\int_0^\infty s^{\frac{p}{2}-1}q^{\frac{p}{2}}J_p\left(2\sqrt{sq}\right)M_{\frac{1}{\gamma}}(s)\,ds \tag{17}$$

where p and q are modulation constants, $\Gamma(\cdot,\cdot)$ is the upper incomplete gamma function [16, eq.(8.350.2)]. By making variable change of $s=x^2$, the BEP is further given by

$$P_e=\frac{1}{2}-\frac{1}{\Gamma(p)}\int_0^\infty x^{p-1}q^{\frac{p}{2}}J_p\left(2\sqrt{q}x\right)M_{\frac{1}{\gamma}}\left(x^2\right)dx$$

$$=\frac{1}{2}-\frac{\xi^2}{2\Gamma(p)\Gamma\left(m_{s,1}\right)\Gamma\left(m_{s,2}\right)\Gamma\left(m_{s,3}\right)\Gamma(a)\Gamma(b)}$$

$$\times H_{2,(2:1),0,(2:4)}^{1,2,0,2,4}\left[\begin{matrix}\frac{\beta_{s,1}}{\beta_{s,2}\beta_{s,3}q}\\\frac{(hab)^r}{\mu_r q}\end{matrix}\middle|\begin{matrix}(p,1),(0,1)\\\left(1-m_{s,2},1\right),\left(1-m_{s,3},1\right);\left(\xi^2+1,r\right)\\-\\\left(m_{s,1},1\right),(0,1);\left(\xi^2,r\right),(a,r),(b,r),(0,1)\end{matrix}\right] \tag{18}$$

4. Simulation results

This section prepares to confirm the analysis by simulation results, which are meticulously designed to convince readers. Assume that the channel gain of each link is normalized to unit one. For RF links, the fading parameters are set to $m_{s,1}=3.3$ and $m_{s,2}=1.1$,

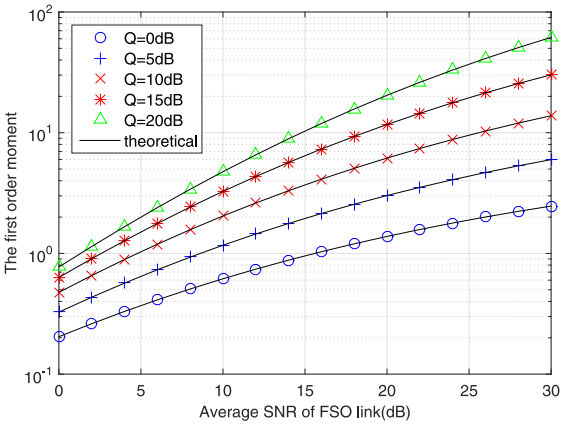

Fig. 2. The first order moment of SNR with IM/DD scheme, $\xi = 1.1$.

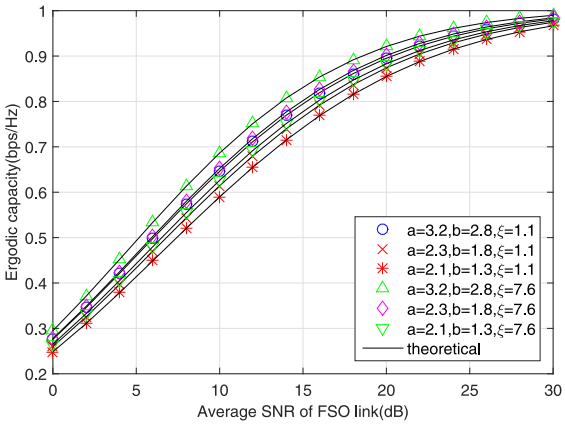

Fig. 3. The ergodic capacity with heterodyne detection, $Q = 5$ dB.

respectively. The number and fading parameters of interfering signals are assumed to be $I = 2$ and $m_{s,3} = 1.5$, respectively. In order to illustrate the applicability of theoretical analysis to arbitrary parameters, here non-integer parameters are specifically selected, because the simulation of integer parameters is relatively simple. Finally, all simulation results are the statistical averages of 6 250 000 experiments, which are enough to produce statistically significant values.

Fig. 2 shows the performance of the first moment of the equivalent SNR under different interference thresholds with IM/DD scheme $r = 2$ and large pointing error $\xi = 1.1$, which are typical values taken from other Refs. [6,7]. As expected, the simulation results coincide with the exact expressions perfectly, which proves the success of the reciprocal SNR moment generating function technique, indicating that the theoretical value can be used to predict and evaluate the network behavior before data transmission. More importantly, Eq. (12) expressed as a Fox's H function is applicable to any fading parameter m and the number of interference signals. However, in [2,3], it is mandatory to require integer parameter m in Nakagami environments, which undoubtedly impose restrictions on the applicable scenarios of the analysis, resulting in certain limitations.

Fig. 3 draws the ergodic capacity of heterodyne detection when the primary user can withstand the interference threshold of no more than $Q = 5$ dB. Different Q values reflect the different quality of service requirements of the primary network. It can be seen from the figure that the ergodic capacity is affected by both atmospheric turbulence and pointing error. Weak atmospheric turbulence condition significantly improve the ergodic capacity, while strong turbulence hinders the propagation of optical signals. For example, it is seen from Fig. 3 that the weak turbulence in case ($a = 3.2, b = 2.8$) obviously achieves a higher capacity than strong scenario in case ($a = 2.3, b = 1.8$).

Fig. 4 presents the ergodic capacity of the hybrid FSO and RF system under different interference levels. The behavior of the ergodic capacity in low interference threshold can be categorized into two parts. Before 25 dB, the ergodic capacity increases rapidly as the SNR increases. After 25 dB, it leads to a capacity floor due to the interference level limitation. The smaller the interference threshold is, the easier the capacity will be saturated. This is because the lower tolerance of the primary user strictly limits the transmission behavior of the secondary user.

Fig. 5 illustrates the BEP under different atmospheric and pointing error conditions. Similar to the above figure, saturation also occurs in Fig. 5 because a relative small interference threshold ($Q = 5$ dB) is chosen to observe the influence of SNR of FSO link.

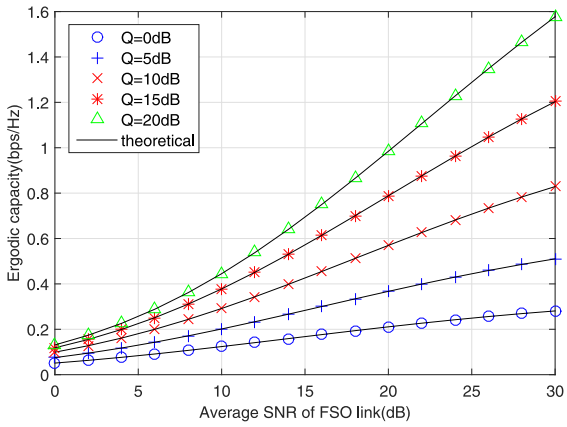

Fig. 4. The ergodic capacity with IM/DD scheme under different interference threshold, $\xi = 1.1$.

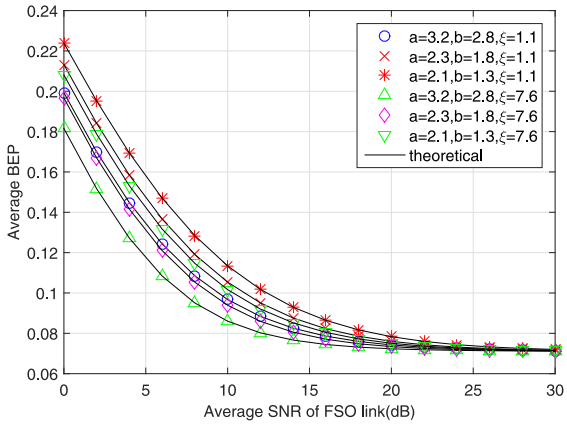

Fig. 5. The average BEP with heterodyne detection, $Q = 5$ dB.

Therefore, the BEP shows a downward trend across the SNR range from 0 dB to 20 dB of FSO link. But when the SNR exceeds 20 dB, the average BEP stops dropping and reaches saturation. This phenomenon illustrates the limiting effect of the interference threshold on the secondary users. When the transmission power of the secondary user increases to a certain value, the BEP keeps unchanged.

Finally, the influence of different interference thresholds on the BEP is drawn in Fig. 6. It can be seen from the figure that increasing the interference threshold of primary network helps secondary network improve the BEP performance. For example, a SNR of approximate 30 dB is required to achieve a BEP of 0.1 at $Q = 5$ dB. But the SNR value drops to about 18 dB when interference threshold increases to $Q = 20$ dB.

From the above results, all formulas have been verified to calculate accurate performance of cognitive hybrid RF and FSO cooperative networks. Importantly, the required results are immediately obtained as long as the corresponding network parameters are substituted. In the popularization of computers today, it is not difficult to compile the corresponding programs by using the popular software platform. These formulas are very practical in actual measurement, because they can predict the behavior of the entire network in advance for subsequent data analysis. For example, the ergodic capacity indicates the amount of information that can be transmitted in the channel environment over a period of time. Before sending data, the transmitter can adjust its own transmission rate so that the destination receiver can decode smoothly without a lot of errors. For another example, the average BEP can predict the possible error conditions and provide a basis for reducing the error probability. In general, when the atmospheric turbulence is strong, the data transmission process is greatly affected by the external environment, and then the error probability will rise at this time. These precise formulas can help us accurately grasp the operating status of this network and avoid a large number of low-level repeated experiments, which waste time and energy.

5. Conclusion

This paper has assessed the precise performance of hybrid RF and FSO AF relaying systems under a spectrum sharing technology in cognitive radio environment. The RF links undergo Nakagami-m fading with arbitrary parameter m, while the FSO channel

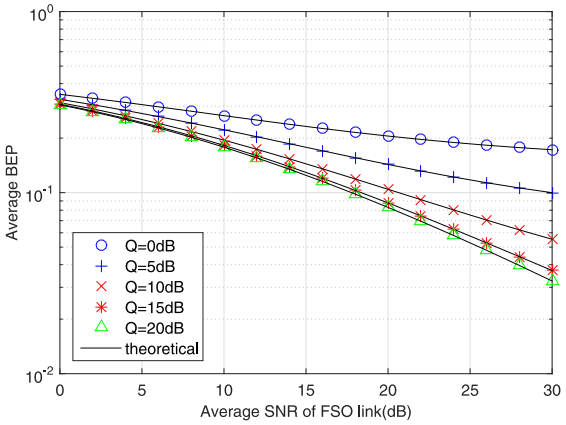

Fig. 6. Average BEP with IM/DD under different interference threshold.

obeys a gamma–gamma distribution with atmospheric turbulence and non zero pointing error. Throwing away the cumulative distribution function and probability density function, new closed-form solutions are provided for moments of the SNR, ergodic capacity, higher-order statistics of the capacity and average BEP by the moment generating function of reciprocal SNR.

Declaration of competing interest

The authors declare that they have no known competing financial interests or personal relationships that could have appeared to influence the work reported in this paper.

Acknowledgment

This work was supported by the National Natural Science Foundation of China under Grant No. 62001201 and under Grant No. 61761030.

References

[1] Saeed Nasir, Celik Abdulkadir, Alouini Mohamed-Slim, Al-Naffouri Tareq Y. Performance analysis of connectivity and localization in multi-hop underwater optical wireless sensor networks. IEEE Trans Mob Comput 2019;18(11):2604–15.
[2] Alathwary Wagdy A, Altubaishi Essam Saleh. On the performance analysis of decode-and-forward multi-hop hybrid FSO/RF systems with hard-switching configuration. IEEE Photon J 2019;11(6):1–12.
[3] Saber Mohammad Javad, Keshavarz Ahmad, Mazloum Jalil, Sazdar Amir Mehdi, Jalil Piran Md. Physical-layer security analysis of mixed SIMO SWIPT RF and FSO fixed-gain relaying systems. IEEE Syst J 2019;13(3):2851–8.
[4] Altubaishi Essam Saleh, Alhamawi Khaled. Capacity analysis of hybrid AF multi-hop FSO/RF system under pointing errors and weather effects. IEEE Photon Technol Lett 2019;31(15):1304–7.
[5] Yi Xiang, Shen Cong, Yue Peng, Wang Yamin, Ao Qingqing, Zhao Peng. Performance analysis for a mixed RF and multihop FSO communication system in 5G C-RAN. J Opt Commun Netw 2019;11(8):452–64.
[6] Abd El-Malek Ahmed H, Aboulhassany Mohamed A, Salhabz Anas M, Zummoz Salam A. Performance analysis and power optimization for spectrum-sharing mixed RF/FSO relay networks with energy harvesting. IEEE Photon J 2019;11(2):1–17.
[7] Arezumand Hamid, Zamiri-jafarian Hossein, Soleimani-nasab Ehsan. Exact and asymptotic analysis of partial relay selection for cognitive RF-FSO systems with non-zero boresight pointing errors. IEEE Access 2019;7:58611–25.
[8] Varshney Neeraj, Jagannatham Aditya K, Varshney Pramod K. Cognitive MIMO-RF/FSO cooperative relay communication with mobile nodes and imperfect channel state information. IEEE Trans Cogn Commun Netw 2018;4(3):544–55.
[9] Arezumand Hamid, Zamiri-Jafarian Hossein, Soleimani-Nasab Ehsan. Outage and diversity analysis of underlay cognitive mixed RF-FSO cooperative systems. J Opt Commun Netw 2017;9(10):909–20.
[10] Varshney Neeraj, Jagannatham Aditya K. Cognitive decode and forward MIMO-RF/FSO cooperative relay networks. IEEE Commun Lett 2017;21(4):893–6.
[11] Khan Muhammad Nasir, Kashif Hasnain, Rafay Abdul. Performance and optimization of hybrid FSO/RF communication system in varying weather. Photon Netw Commun 2021;41(1):47–56.
[12] Kashif Hasnain, Khan Muhammad Nasir, Altalbe Ali. Hybrid optical-radio transmission system link quality: link budget analysis. IEEE Access 2020;8:65983–92.
[13] Arya Sudhanshu, Chung Yeon Ho. Amplify-and-forward multihop non-line-of-sight ultraviolet communication in the gamma-gamma fading channel. J Opt Commun Netw 2019;11(8):422–36.
[14] da Costa Daniel Benevides, Yacoub Michel Daoud. Outage performance of two hop AF relaying systems with co-channel interferers over Nakagami-m fading. IEEE Commun Lett 2011;15(9):980–2.
[15] Li Ruijie, Chen Te, Fan Luhai, Dang Anhong. Performance analysis of a multiuser dual-hop amplify-and-forward relay system with FSO/RF links. J Opt Commun Netw 2019;11(7):362–70.
[16] Gradshteyn IS, Ryzhik IM. Table of integrals, series and products. 7th ed.. Academic Press; 2007.
[17] Kilbas AA, Saigo M. H-transforms: theory and applications. CRC Press; 2004.

[18] Salih Al-Ebraheemy Omer Mahmoud, Salhab Anas M, Chaaban Anas, Zummo Salam A, Alouini Mohamed-Slim. Precise performance analysis of dual-hop mixed RF / unified-FSO DF relaying with heterodyne detection and two IM-DD channel models. IEEE Photon J 2019;11(1):1–22.
[19] Renzo Marco Di, Graziosi Fabio, Santucci Fortunato. A unified framework for performance analysis of CSI-assisted cooperative communications over fading channels. IEEE Trans Commun 2009;57(9):2551–7.
[20] Mathai AM, Saxena RK. The H-function with applications in statistics and other disciplines. John Wiley & Sons; 1978.
[21] Ferdinand Nuwan S, Jayasinghe Upul, Rajatheva Nandana, Latva-aho Matti. Impact of antenna correlation on the performance of partial relay selection. Eurasip J Wirel Commun Netw 2012;2012:1–13.
[22] Yilmaz Ferkan, Alouini Mohamed-Slim. On the computation of the higher-order statistics of the channel capacity over generalized fading channels. IEEE Wirel Commun Lett 2012;1(6):573–6.

Dong Qin received the Ph.D. degree in information and communication engineering from Southeast University, Nanjing, China, in 2016. He joined the School of Information Engineering, Nanchang University, in 2016. His current research interests include the areas of cooperative communication and OFDM techniques.